Contributions of escape depth to photoelectron intensity of a well defined initial state

M. Morgenstern[1], T. Strasser[2], R. Adelung[3], M. Getzlaff[4], L. Kipp[3], M. Skibowski[3], W. Schattke[2], and R. Wiesendanger[1]

[1] *Inst. of Appl. Physics, Hamburg University, Jungiusstraße 11, D–20355 Hamburg, Germany*

[2] *Inst. für Theoretische Physik und Astrophysik, Christian-Albrechts-Universität, Leibnizstraße 15, D-24098 Kiel, Germany*

[3] *Inst. for Exp. and Appl. Physics, Christian-Albrechts-University, Leibnizstraße 19, D-24098 Kiel, Germany*

[4] *Inst. of Appl. Physics, University of Düsseldorf, Universitätsstr. 1, D-40225 Düsseldorf, Germany*

(Submitted 12 March, 2004)

Abstract

Using the adsorbate induced two dimensional electron system on InAs(110) as an initial state, which provides rather small energy and k-space distribution, we measure the photoelectron intensity as a function of photon energy. It oscillates twice between 6 eV and 25 eV having maxima at around 10 eV and 24 eV. Comparison with calculations performed within the one-step model show that the maximum at low energy is due to an overlap of a maximum in the photoelectron escape depth and a maximum of the matrix elements corresponding to the atomic wave functions. In contrast, the maximum at high energy is caused by final states crossing the Γ-point exactly at this energy. The comparison confirms the theoretical prediction that the escape depth at low excitation energies can be significantly modified by band structure effects.

PACS : 79.60.Jv, 73.21.Fg

Typeset using REVTEX

Angle resolved photoelectron spectroscopy (ARUPS) is a standard technique to map the band structure of occupied electronic states. At photoelectron energies from 10 eV to 1 keV, ARUPS is extremely surface sensitive. At higher energies, the information depth is increased and photoemission becomes more bulk sensitive [1]. At lower energies, one generally assumes that the escape depth $\lambda(E)$ increases strongly and monotonically being largely material independent [3]. However, recent theory predicts that $\lambda(E)$ can oscillate at these energies [2]. This is explained by a significant increase of λ at critical points of the band structure. In order to measure the effect, one has to consider that the photoelectron intensity depends also on matrix elements and the distribution of final states [4]. To disentangle the different contributions, it is useful to start with a well defined initial state. Here, we use the Fe induced 2D electron system (2DES) close to the surface of InAs(110) [5,6]. From comparison with one-step photoemission calculations, we indeed deduce an oscillation of $\lambda(E)$ at low kinetic energies.

The advantages of our initial state are the following:

1. The 2DES is energetically separated from all other states of the sample, since it exists in the bulk band gap [5,6]. This eliminates influences of energetic overlap with photoelectrons from other bands.

2. The 2DES belongs to an electronically simple s-like and nearly parabolic band [7], which reduces the complexity of matrix element effects.

3. The 2DES electrons are restricted to $\vec{k} \simeq \vec{0}$. This reduces the number of relevant final states significantly. Parallel to the surface (x, y) only the inner 0.2 % of the Brillouin zone are occupied [5]. Perpendicular, the self-consistently calculated wave function [8] is very close to $\Psi_0(z) \simeq \sqrt{b^3/2} \cdot z \cdot e^{-bz/2}$ ($b = 3.3 \cdot 10^8$ m^{-1}) [9]. Its k_z-distribution is given by the Fourier transformation exhibiting 90 % of the intensity within 0.1 Å^{-1} around the Γ-point.

4. The surface has a very low defect density [10] which reduces contributions from elastic

scattering [11].

5. The z-extension of the 2DES of 5 nm [5] is much less than the photon wave length ($\lambda \geq 40$ nm) allowing to treat the electric field of the light as constant.

To illustrate these advantages, we use the one-step model and the knowledge that final vacuum states decay exponentially into the sample with decay length $\lambda(E)$ [2]. This allows to derive a rather simple expression for the photoelectron intensity per photon starting with [4]:

$$I(E) \propto \rho_f(E) \cdot |M_B(E)|^2 \cdot |\int_0^\infty \Psi_0(z) \cdot e^{ik_z(E)z - z/\lambda(E)} dz|^2$$

Here, $\rho_f(E)$ is the relevant density of final vacuum states, $M_B(E)$ is the matrix element, and $k_z(E)$ is the wave vector of the final states inside the sample. $\Psi_0(z)$ is given above with $b = (16.5 \cdot \pi m^\star e^2 N_{2DES}/\epsilon\epsilon_0 \hbar^2)$ depending on effective mass $m^\star$, dielectric constant ϵ and the known electron density of the 2DES N_{2DES} [9]. The integral can be solved resulting in

$$I(E) \propto \frac{\rho_f(E) \cdot |M_B(E)|^2}{(k_z(E)^2 + (b/2 + 1/\lambda(E))^2)^2} \tag{1}$$

A single k_z-value is assumed, but contributions from different k_z can be simply summed up. Since $b/2$ and $1/\lambda(E)$ are small with respect to the Brillouin zone boundary at 14.6/nm, transitions close to $k_z = 0$ are strongly favored. In addition, transitions with large $M_B(E)$, large $\rho_f(E)$ and/or large $\lambda(E)$ are most intense.

To calculate Φ_{LEED}, the final state of photoemission, within the one-step model, one uses the time inverse of a low energy electron diffraction (LEED) state, whose asymptotic is matched to the solution of the complex bulk band structure [12]. To deduce $\lambda(E)$, the different Φ_{LEED} are fitted to $e^{-z/\lambda(E)}$. We find $\lambda \in [0.9 \text{ nm}, 1.7 \text{ nm}]$, i.e. $1/\lambda > b/2$. Thus, the contribution of $\lambda(E)$ is always relevant, if $k_z(E)$ is small.
The initial states are represented by the half-space Green's function, given as a layer resolved contribution of atomic orbitals Ψ_i. The basis set consists of 5s and 5p orbitals for In and 4s and 4p orbitals for As. Matrix elements $M_B(E)$ are calculated as

$< \Phi_{LEED}(E_{\mathrm{fin}}, \vec{k}_{||})|\vec{A}_0 \cdot \vec{p}\,|\Psi_i >$ with the light induced vector potential $\vec{A}_0$ kept constant. Polarization and incident angle of the light are taken as in the experiment. Since we, thus, have calculated $M_B(E)$, $\lambda(E)$ and the band structure of final states, we can disentangle the different contributions to $I(E)$.

The ARUPS experiments are performed at the HONORMI beamline of HASYLAB using the ASPHERE analyzer [13]. The light is p-polarized with an incident angle of 30° towards [001]. The energy resolution of the experiment is 20 meV and the angular resolution 0.25° in one and 0.45° in the other direction. The Fermi level E_F is determined on a clean Ta-foil with an accuracy of 5 meV. Degenerate n-InAs ($N_{\mathrm{D}} = 1.1 \times 10^{16}/\mathrm{cm}^3$) is cleaved in-situ at a base pressure of 10^{-8} Pa. This leads to nearly defect free InAs(110) exhibiting flat band conditions up to the surface [14]. To induce the 2DES, 4.5 % of an Fe monolayer is deposited. The coverage is determined by a quartz balance and cross-checked by STM. The surface bands shift downwards by 300 meV [5]. One gets an accumulation layer (2DES) with $N_{2DES} = 2 \cdot 10^{12}$ cm^{-2} as confirmed by scanning tunneling spectroscopy [6]. This gives $b = 3.3 \cdot 10^8$ m^{-1} determining $\Psi_0(z)$ completely.

Fig. 1a shows an energy scan of the 2DES intensity at photon energy $h\nu = 10$ eV and $\theta = 0°$. Fig. 1b shows the angular scans recorded at different $E - E_F$. A linear background caused by second order light is subtracted. The straightforward fit of the data [5] is shown as a solid line for Fig. 1a and in Fig. 1c. for Fig. 1b. The fit takes into account the known energy and angular resolution of the experiment [13], the known band dispersion of the InAs conduction band [15] and the known temperature $T = 300$ K. It assumes a constant $M_B(E)$, $\lambda(E)$ and $\rho_f(E)$ as expected in the small energy and angular (k-space) region of the data. The first two fitting parameters are the subband energies E_i, which are confirmed by scanning tunneling spectroscopy [6]. An adjustment of the total intensity by a single factor is still necessary. This factor accounts for $M_B(E)$, $\lambda(E)$ and $\rho_f(E)$ and for the instrumental efficiency. It is the only free parameter and nicely reproduces all results in Fig. 1a and b.

Fig. 2a shows the 2DES peak at different $h\nu$. The data are normalized to the photon flux calibrated by a Au film prior to the experiments. Therefore, the quantum efficiency of the Au diode is considered [16]. During the experiments, the positron current in the synchrotron is used to link the calibrated to the actual photon flux. The data of Fig. 1 and 2 are from the same sample, but several samples with the same coverage are used and the normalized intensity is reproducable within $10-20$ %. Obviously, the peak intensity depends non-monotonously on $h\nu$. Before we compare with calculations, we have to consider the fact that the angular width of the peak also depends on $h\nu$. This is demonstrated in Fig. 2c. The reason for the reduced width with increasing $h\nu$ is simply that $k_{||} \propto \sin\theta \cdot \sqrt{E_{\rm kin}}$. Thus, the same k-space distribution of the 2DES leads to a smaller $\Delta\theta$ at higher $E_{\rm kin}$ ($h\nu$) increasing the ARUPS collection efficiency. However, the effect can be straightforwardly calculated by the fit model described above. The normalized peak intensity devided by the collection efficiency is shown for four data sets in Fig. 3a. The statistical error bar is 10 % at $h\nu = 10 - 23$ eV, 20 % at higher and 40 % at lower $h\nu$. The data show a pronounced peak at $h\nu = 10$ eV, a tiny peak at 17.5 eV and a broad peak around 24 eV. The data are largely reproducible, except that the peak at 24 eV is 25 % larger in one data set. Note that $I(E)$ increases by a factor of six between 8 eV and 10 eV.

The measured $I(E)$ data will be compared with calculated $I(E)$ data. Therefore, the half-space Green's function for the initial states is calculated for $\vec{k}_{||} = 0$ and for an energy at the bottom of the InAs conduction band. Although k_z is not a quantum number in the half-space Green's function, the restriction to the bottom of the conduction band requires $k_z \simeq 0$ as in the experiment. A free parameter in the calculation is the position of the matching plane between the vacuum LEED asymptotic and the complex states of the crystal. It is chosen at 1.4 Å above the first atom, but it is checked that the results do not change significantly from 1 Å to 2 Å. Figure 3b shows the calculated I(E) curve. It also exhibits a sharp peak at $h\nu = 10.5$ eV and a broad peak around $h\nu = 24$ eV. The peak heights are nearly identical to the experiment. The tiny peak at $h\nu = 17.5$ eV faintly appears as a broad shoulder within the calculation. Generally the experimental results are nicely reproduced by the one-step model setting the base for a deeper analysis.

Fig. 4 shows the different contributions to $I(E)$. The $\lambda(E)$ curve derived from the $e^{-z/\lambda}$ fits to the final states is plotted in Fig. 4a. It shows a maximum between 7 eV and 11 eV, where λ is enhanced by up to 70 %. Putting $\lambda(E)$ into eq. (1) using $k_z = 0$, $b = 3.3 \cdot 10^8$/m, $M_B(E) =$ const, and $\rho_f(E) =$ const, results in an $I(E)$ peak six times larger than the surrounding. This height is indeed found in the $I(E)$ data, but the $\lambda(E)$ peak is at 8 eV and the $I(E)$ peak is at 10 eV. Thus, other factors must contribute. Fig. 4b shows $|M_B(E)|$, which is calculated separately for each layer. Only the As s-orbital is considered, since it strongly dominates at the InAs conduction band edge [7]. A strong maximum appears around 12 eV for all layers, while a smaller maximum at 7 eV appears only from the second layer on. The maximum at 12 eV is three times larger than the surrounding, which would lead to an $I(E)$ peak nine times larger than the surrounding again comparable to the $I(E)$ data. However, the $|M_B(E)|$ peak is at higher energy than the $I(E)$ peak. Thus, it also cannot explain it exclusively. Finally, the k_z distribution of the final states has to be considered. Fig. 4c shows the complex band structure of InAs(110) in the direction perpendicular to the surface. The bulk states of an infinite crystal are displayed as thin lines, while some of the complex states decaying into the semi-infinite crystal are drawn as thick lines. Only complex states with a significant coupling to the vacuum LEED asymptotic are plotted. The vertical bars mark the intensity of coupling to the vacuum state. Thus, the largest bar indicates the dominating wave vector of the final state inside the crystal. Coming back to eq. (1), the different k_z contributions of the final state have to be summed up. Obviously, the final states do neither show a strong ($k_z = 0$)-contribution at 10 eV nor an increased density of states, i.e. the same number of bands with similar coupling strength to vacuum appear across the maximum. Thus, without performing the intricate calculation summing up over all k_z-contributions, we can state that the peak at 10 eV is due to an overlap of a peak in $M_B(E)$ and in $\lambda(E)$, but none of the two contributions can explain it exclusively.

The second $I(E)$ peak at $h\nu = 24$ eV is three times higher than the surrounding. It appears

neither in the $\lambda(E)$- nor in the $|M_B(E)|$-curves. Again the number of complex bands and their coupling strength to vacuum is basically constant at 24 eV. Moreover, the dispersion of the bands is rather linear, i.e. $\rho_f(E)$ is constant. However, three complex bands including the one with the strongest coupling cross the Γ point exactly at 24 eV giving rise for direct transitions. We conclude that the $I(E)$ peak is a consequence of $k_z \simeq 0$ of the final state. In the experiment, the overlap of the oscillating final state with $\Psi_0(z)$ of the 2DES explains the peak, while in the calculation the restriction of initial states to $k_z \simeq 0$ is responsible. Thus, the peaks at 10 eV and 24 eV have completely different origin. One is due to a large escape depth and an enhanced matrix element and the other one is due to a k_z matching of the final states to the initial state.
Note, finally, that the $I(E)$ data are only explained, if a maximum of $\lambda(E)$ is assumed. This contradicts the convential knowledge that $\lambda(E)$ is a smooth curve with a single minimum at 50 eV [3]. However, it confirms previous calculations on GaAs(110) exhibiting a similar maximum [2]. The reason for the increased λ at 8 eV is not completely clear, but the bulk band structure (thin lines) exhibits a large number of extrema around 8 eV, i.e. the bulk density of states is large. Consequently, the complex states can couple more effectively to real states increasing their decay length. Interestingly, the high-T_c superconductor Bi2212 also shows a $\lambda(E)$ maximum (at 10 eV) [17]. However, this maximum is explained by the different plasmons of the layered material.

In summary, we measured the photoelectron intensity of a well defined initial state given by the Fe induced 2DES on InAs(110). The $I(E)$ curve is reproduced by a calculation within the one-step model taking the details of the experiment into account. An analysis of the calculation reveals that a peak at $h\nu = 10$ eV is due to an overlap of an increased photoelectron escape depth and an enhanced matrix element. Another peak at $h\nu = 24$ eV is due to a k_z matching of initial and final states. The measurements confirm that the electron escape depth of InAs(110) is not a smooth function of energy but exhibits a pronounced maximum around $h\nu = 8$ eV.

We thank K. Rossnagel, O. Seifarth and J. Klijn for technical assistance and acknowledge financial support from SFB 508/B4 and BMBF project 05 KS1FKB.

REFERENCES

[1] A. Sekiyama *et al.*, Nature **403**, 396 (2000); Y. Saitoh *et al.*, J. Synchrotron Rad. **5**, 542 (1998).

[2] C. H. Solterbeck *et al.*, J. Electr. Spectr. Rel. Phen. **101-103**, 473 (1999).

[3] G. A. Somorjai, *Chemistry in Two Dimensions: Surfaces* (Ithaca, Cornell, 1981); G. Ertl *et al.*, *Low Energy Electrons and Surface Chemistry* (VCH, Weinheim, 1985).

[4] S. Hüfner, *Photoelectron Spectroscopy* (Springer, Berlin 1995).

[5] M. Morgenstern *et al.*, Phys. Rev. B **61**, 13805 (2000).

[6] M. Morgenstern *et al.*, Phys. Rev. Lett. **89**, 136806 (2002).

[7] J. L. Alves *et al.*, Phys. Rev. B **44**, 8188 (1991); B. Engels *et al.*, Phys. Rev. B **58**, 7799 (1998); J. Klijn *et al.*, Phys. Rev. B **68**, 205327 (2003).

[8] M. G. Betti *et al.*, Phys. Rev. B **63**, 155315 (2001); V. Aristov *et al.*, Surf. Rev. Lett. **5**, 235 (1998).

[9] T. Ando *et al.*, Rev. Mod. Phys. **54**, 437 (1982).

[10] M. Morgenstern *et al.*, J. Electr. Spectr. Rel. Phen. **109**, 127 (2000).

[11] J. Zemek *et al.*, Surf. Sci. **473**, 8 (2001); I. S. Tilinin, Phys. Rev. B **53**, 547 (1996).

[12] J. Henk *et al.*, Phys. Rev. B **39**, 13286 (1989); **47**, 2251 (1993).

[13] K. Rossnagel *et al.*, Nucl. Instrum. Methods Phys. Res. A **467-8**, 1485 (2001).

[14] C. B. M. Andersson *et al.*, Surf. Sci. **398**, 395 (1998).

[15] U. Merkt *et al.*, Phys. Rev. B **35**, 2460 (1987).

[16] K. U. Gawlik, Dissertation (Kiel,1996) i

[17] M. R. Norman *et al.*, Phys. Rev. B **59**, 11191 (1999).

FIGURES

FIG. 1. (a) Energy scan of 2DES peak and fit (see text) at $h\nu = 10$ eV, $\theta = 0°$, $E_{\text{pass}} = 4$ eV; E1, E2: subband energies. (b) Angular scans of 2DES peak at different $E - E_F$, $h\nu = 10$ eV, $E_{\text{pass}} = 4$ eV. (c) Fit curves to (b) with same fit parameters as in (a); same symbols are used in (b) and (c) as marked in between.

FIG. 2. (a), (b) Energy scans of 2DES peak at different $h\nu$ as indicated, $E_{pass} = 20$ eV, $\theta = 0°$; data are scaled to photon fluence and offset as marked by horizontal lines. (c) Angular scans of 2DES peak at different $h\nu$ as indicated, $E_{\text{pass}} = 4$ eV, $E - E_F = -50$ meV; data are scaled to the same height at $\theta = 0°$; the horizontal line FWHM is at half maximum.

FIG. 3. (a) 2DES peak intensity normalized to the photon fluence and to the angular collection efficiency of the analyzer; different E_{pass} are indicated. (b) Calculated photoelectron intensity in normal emission using the initial states at the bottom of the conduction band of InAs(110); calculation performed according to [12].

FIG. 4. (a) Calculated escape depth λ as a function of energy. (b) Matrix elements corresponding to the As s-orbitals of the initial states displayed for different layers from the surface as indicated. (c) Complex band structure of InAs(110) perpendicular to the surface; thin lines are real states of the infinite crystal, thick lines are complex states of the semi-infinite crystal; vertical bars mark the strength of the coupling of complex states to vacuum states; only states with significant coupling are plotted; E_{final} at the lower bar is given with respect to the valence band maximum.

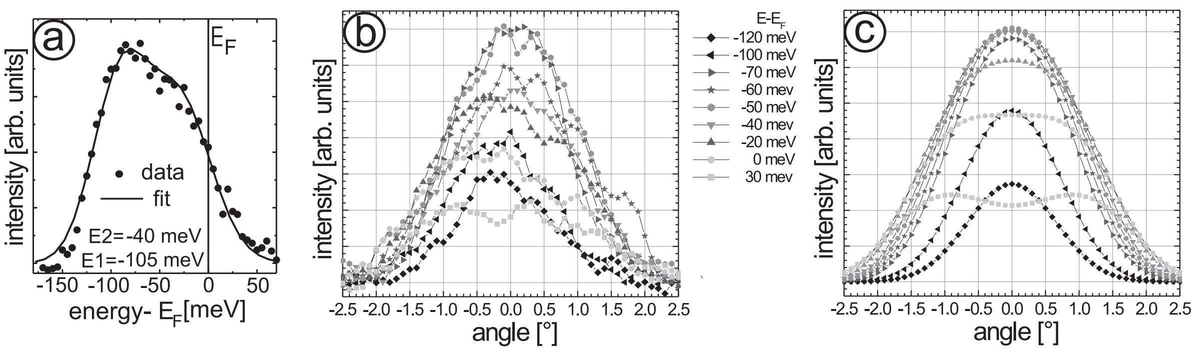

a
b
c
intensity [arb. units]
energy- E_F [meV]
E_F
data
fit
E2=-40 meV
E1=-105 meV
-150
-100
-50
0
50
angle [°]
-2.5 -2.0 -1.5 -1.0 -0.5 0.0 0.5 1.0 1.5 2.0 2.5
E-E_F
-120 meV
-100 meV
-70 meV
-60 mev
-50 meV
-40 meV
-20 meV
0 meV
30 mev

Fig. 1

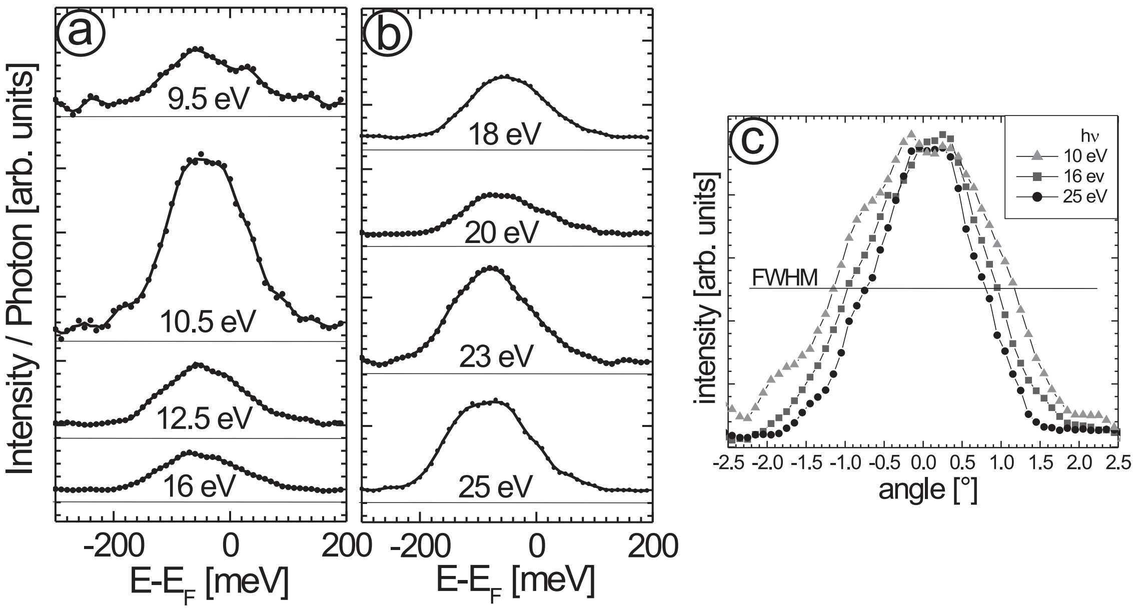
a
b
c
9.5 eV
10.5 eV
12.5 eV
16 eV
18 eV
20 eV
23 eV
25 eV
Intensity / Photon [arb. units]
-200
0
200
E-E_F [meV]
hν
10 eV
16 ev
25 eV
FWHM
intensity [arb. units]
-2.5 -2.0 -1.5 -1.0 -0.5 0.0 0.5 1.0 1.5 2.0 2.5
angle [°]

Fig. 2

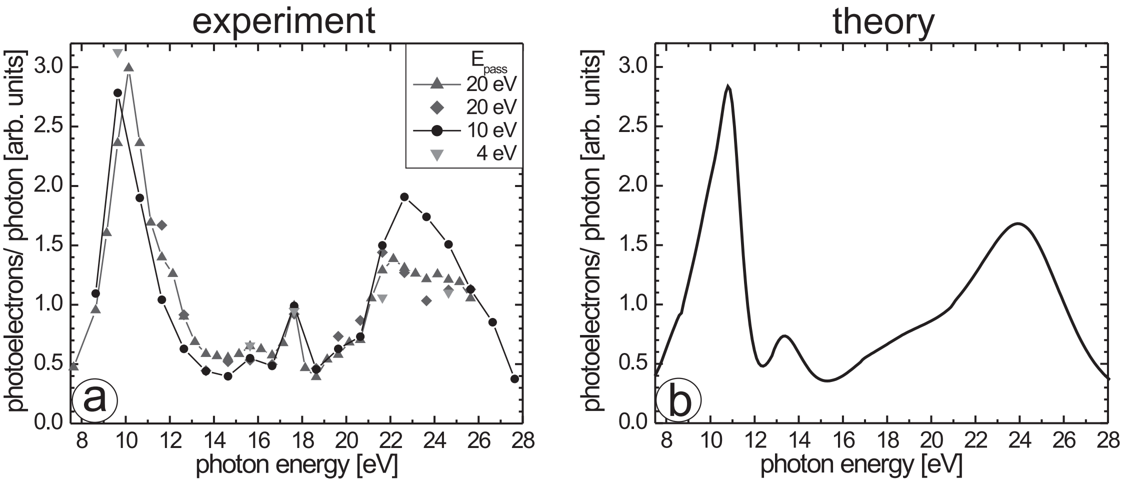
experiment
theory
E_{pass}
20 eV
20 eV
10 eV
4 eV
a
b
photoelectrons/ photon [arb. units]
photon energy [eV]

Fig. 3

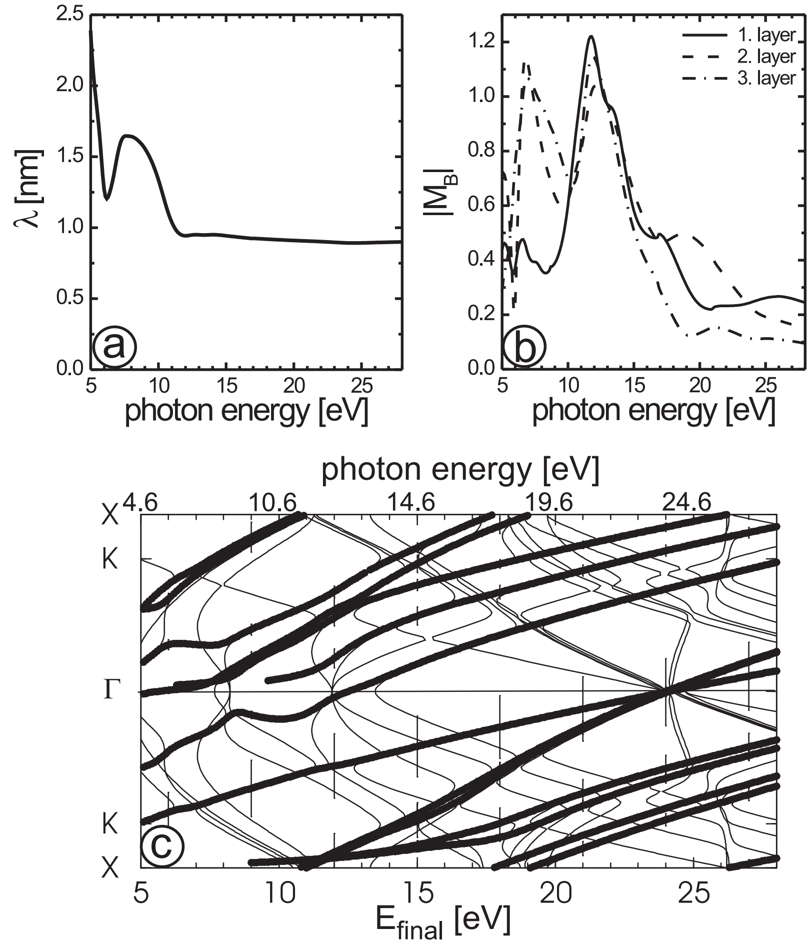

a
b
c
λ [nm]
|M_B|
photon energy [eV]
1. layer
2. layer
3. layer
X
K
Γ
K
X
E_final [eV]

Fig. 4